

# Design and Analysis of Enhanced Harris Hawks Optimization-Tuned Type-2 Fuzzy Fractional Proportional Integral Derivative Controller for the Frequency Control of Microgrid System

Gauri Sahoo<sup>1</sup>, Rabindra Kumar Sahu<sup>1</sup>, Pratap Chandra Pradhan<sup>2</sup>, Sidhartha Panda<sup>3</sup>

<sup>1</sup>Department of Electrical & Electronics Engineering, Veer Surendra Sai of Technology (VSSUT), Odisha, India

<sup>2</sup>Department of Electrical Engineering, DRIEMS, Cuttack, Odisha, India

<sup>3</sup>Department of Electrical Engineering, Veer Surendra Sai of Technology (VSSUT), Odisha, India

**Cite this article as:** G. Sahoo, R. Kumar Sahu, P. Chandra Pradhan and S. Panda, "Design and analysis of enhanced harris hawks optimization-tuned type-2 fuzzy fractional proportional integral derivative controller for the frequency control of microgrid system," *Electrica*, 23(2), 294-309, 2023.

## ABSTRACT

The imprecise character of renewable energy sources and fluctuations in load demand makes the modern microgrids complicated thus introducing frequency deviations. To preserve the power balance between source and load by implementing a suitable controller for frequency control, in the present study, a type-2 fuzzy fractional order proportional integral derivative structure is suggested for frequency regulation of the microgrid system. The frequency control of microgrid system is carried out by a type-2 fuzzy fractional order proportional integral derivative controller tuned by the enhanced Harris Hawks optimization method. The effectiveness of the enhanced Harris hawks optimization is evaluated in comparison with Harris Hawks optimization, gravitational search algorithm, genetic algorithm, and Grey wolf optimization. The dominance of enhanced Harris hawks optimization-based type-2 fuzzy fractional order proportional integral derivative is established by evaluating its performances with proportional integral derivative and fuzzy proportional integral derivative controllers for different case studies of normal and increased/unavailability of renewable energy source generation. Furthermore, an uncertainty study is done to investigate the performance of suggested controllers under parameter variations. Finally, the analysis is expanded to a two equal-area non-reheat/reheat thermal systems and compared with recently published approaches.

**Index Terms**—EHHO algorithm, frequency regulation, microgrid, renewable energy sources, T2FFOPID

## Corresponding author:

Rabindra Kumar Sahu

## E-mail:

rksahu\_ee@vssut.ac.in

**Received:** July 21, 2022

**Revised:** September 27, 2022

**Accepted:** October 26, 2022

**Publication Date:** December 6, 2022

**DOI:** 10.5152/electrica.2022.22123



Content of this journal is licensed under a Creative Commons Attribution-NonCommercial 4.0 International License.

## I. INTRODUCTION

Considering the higher demand for electrical power, the increasing cost of electricity transmission, and the rising trend of environmental pollution due to the use of conventional fuels, renewable energy sources (RESs) impart a better choice for modern electrical power utilities. On the other hand, RESs like solar photovoltaic (PV) and wind turbine generators (WTG) are very erratic due to their dependency on solar position and weather conditions, respectively. The unpredictable nature of RESs and sudden increase in power demand cause variation in the grid frequency. In a microgrid system (MGS), various energy-storing devices like batteries, capacitors, flywheels, etc. are integrated to gather the surplus power, from the RESs, as well as to deliver the deficit energy, when generated power is lower than the load demand [1-3]. An appropriate generation control scheme is required for supervising this behavior precisely and taking corrective measures.

Earlier, researchers have investigated different ideas to control the frequency of MGS. In most cases, conventional controllers are implemented for frequency regulation (FR) although their efficacy is affected due to parameter variations and the presence of non-linearity. This difficulty in dealing with uncertainties can be mitigated by using a fuzzy logic controller (FLC) supported by a suitable optimization scheme. Currently, various FLC-aided schemes like tuned fractional order fuzzy PID (FOFPID) have been recommended [4, 5]. A modified black hole algorithm has been applied to optimize a fractional order fuzzy PD+I controller for islanded MGS [6]. For frequency control of MGS with electrical vehicles (EVs), a T2FPI controller optimized by modified harmony search algorithm was suggested in [7] and FOFPID based on MBHA was proposed in [8]. An improved JAYA (IJAYA) tuned fuzzy cascaded configuration for secondary frequency control has been proposed in [9]. The conventional PID with fuzzy logic controller seems to be useful for improving performance in numerous load frequency control studies [10,11]. Under larger uncertainties, it

may not give the required performances. However, a type-2 fuzzy PID structure with a dual membership function (MF) conversely gives an upgraded performance [12]. In this study, frequency control of MGS using a type-2 Fuzzy FOPID structure is suggested. Type-2 fuzzy fractional order PID (T2FFOPID) controller has been proposed which consists of a type-2 fuzzy logic controller (FLC) and FOPID. Conventional PIDs are usually ineffectual if time delay systems and uncertainties are involved. On the contrary, the type-2 FLC can deal with uncertainties and non-linearity. The proposed T2FFOPID structure takes the benefits of the capabilities of a FLC and FO control system to remove the steady-state error with improved performance. With T2FFOPID structure, because of the ability to handle nonlinearity, quick response and an effective control action can be realized.

Researchers around the world are applying soft computing algorithms for selecting gain parameters of the controller. It is observed that all algorithms provide an acceptable result to a certain extent; however, in resolving every optimizing task always, a specific method does not give better results than others. Thus, novel techniques are proposed for specific problems. Numerous amendments to the existing methods such as improved whale optimization algorithm (IWOA) [13], improved grey wolf optimization (IGWO) [14], binary butterfly optimization [15], hybrid WOA with simulated annealing [16], hybrid gravitational search and pattern search [17], cosine-adopted modified WOA [18], etc. have been suggested to improve the algorithm performance. There is no free lunch because no single method fits suitable for every problem, and hence, new methods should be attempted for each problem. Harris hawks optimization (HHO) technique inspired by the unique and effective method of hunting by Harris hawks is the most recently projected method. The supremacy of HHO over many similar optimization techniques has been reported in [19, 20]. In [21], the application of HHO to optimize a PID controller for speed control of a DC motor has been done. The authors have demonstrated that HHO/PID controller is more efficient than atom search optimization (ASO), grey wolf optimization, and sine-cosine algorithm-based PID controllers. In [22], HHO has been applied to design a PID controller for pitch angle control of aircraft system and compared the results with the salp swarm algorithm and ASO-tuned PID controllers. In [23], the application of HHO algorithm to design a FOPID controller for a vehicle cruise control system has been performed and the outcomes are equated with some published approaches. The application of HHO for training multi-layer perceptron and its superiority over the sine cosine algorithm has been reported in [24].

In HHO, the escaping energy of prey ( $E$ ) reduces linearly control switching during the searching (exploration) and operating (exploitation) stages. The exploration phase is executed for  $E \geq 1$ ; otherwise, the exploration stage is performed neglecting the equilibrium amid them to yield an optimum solution. This limitation is overcome by maintaining a perfect equilibrium among the search stages to get a better result in enhanced HHO (EHHO). Moreover, the appropriate selection of scaling factors (SFs) evades the random shift of search agents during the search process's initial phases.

The novelties and contributions of the presented work are explained below:

- i) A robust T2FFOPID controller is proposed to preserve frequency steadiness in MGS.
- ii) EHHO method is suggested for preserving the appropriate balance between exploration and exploitation. Also, the

technique's effectiveness is enhanced by employing an appropriate selection of scaling factors (SFs).

- iii) The dominance of EHHO over the HHO is shown in addition to other acknowledged methods like GA, Particle Swarm Optimization (PSO), GSA, and GWO.
- iv) The efficiency of the suggested T2FFOPID controller is confirmed by suitable comparative analysis with Fuzzy PID (FPID) and PID.
- v) The effectiveness of the T2FFOPID controller is confirmed by some published approaches.

## II. ENHANCED HARRIS HAWKS OPTIMIZATION

The Harris's hawks are well recognized for hunting cooperatively in groups. Also, according to the prey's behavior, Harris's hawks change their strategies for foraging and besieging. Such a unique, collaborative, and effective method of hunting became the motivation for HHO [19]. Various steps of HHO are described below [25].

### A. Exploration Mode

The individual hawks of HHO act as search agents. Sometimes, it becomes difficult for the hawks to locate the prey and then look into the areas for hours for searching the prey. Such behavior of Harris's hawks in HHO is called exploration mode. Hawks are chosen as possible solutions and probable prey as the best solution. While resting, hawks search the prey with two strategies. Either the hawks can rest in a position close to other members (equated in (1) for  $p < 0.5$ ) or rest arbitrarily on a location (equated in (1) for  $p \geq 0.5$ ). The best outcome in each cycle is considered as an objective rabbit or prey. It executes a two-fold method of similar importance to explore the search region. These steps are explained in (1) as follows:

$$H(k+1) = \begin{cases} H_{rand}(k) - c_1 |H_{rand}(k) - 2c_2 H(k)| & p \geq 0.5 \\ (H_{rabbit}(k) - H_m(k)) - c_3 (lb + c_4 (ub - lb)) & p < 0.5 \end{cases} \quad (1)$$

where for the present iteration;  $H_{rabbit}(k)$  is the prey's position,  $H(k)$  is the hawk's position,  $c_1, c_2, c_3, c_4, p$  are random parameters in the interval (0, 1), the search limits are  $ub$  and  $lb$ ,  $H_{rand}(k)$  is a hawk's position selected randomly, and  $H_m(k)$  is average position of entire hawks in  $k^{th}$  iteration.  $H(k+1)$  is the hawk's position vector in the subsequent phase. The mean position of the hawk,  $H_m(k)$ , is calculated in (2) as follows:

$$H_m(k) = \frac{1}{N} \sum_{i=1}^N H_i(k) \quad (2)$$

Where,  $N$  is the total number of hawks and  $H_i(k)$  is the individual hawk's position in  $i^{th}$  iteration.

### B. Crossover from Exploration to Exploitation Stage

During the hunt, the prey's escaping energy decreases as given in (3)

$$E = 2E_0 \left(1 - \frac{k}{l}\right) \quad (3)$$

where  $E$  is prey's escaping energy,  $E_0$  is energy at the initial stage, and  $l$  is no. of iterations.  $E_0$  vary randomly in the restrictions  $(-1, 1)$  at each  $k$  as given in (4)

$$E_0 = rand(-1, 1) \quad (4)$$

For  $|E| \geq 1$ ,  $|E| \geq 1$  is the exploration period that has taken place and when  $|E| < 1$   $|E| < 1$ , the exploitation period happens.

### C. Exploitation Phase

In the exploitation phase, hawks jump surprisingly on the targeted prey. Here, parameter  $e$  is illustrated as the prey's chance of escaping from the hawk's attack. For  $e < 0.5$ , the prey successfully escapes, whereas, for  $e \geq 0.5$ , the prey gets captured. Depending upon escaping pattern and energy of the prey, hawks take on the besiege strategy. Finally, by repeated pounces, the hawks fetch the prey that was exhausted and then make a hard besiege to hunt the prey successfully. Depending upon the escaping energy level of the prey and its possibilities of escaping from the striking hawks, besiege and hunt methods are divided into four states as follows:

#### 1) Soft Besiege Mode

For  $e \geq 0.5$  and  $|E| \geq 0.5$ , the prey has sufficient energy to escape and make random confused movements but could not get away as given in (5-6):

$$H(k+1) = \Delta H(k) - E |R_j H_{rabbit}(k) - H(k)| \quad (5)$$

$$\Delta H(k) = H_{rabbit}(k) - H(k) \quad (6)$$

Where,  $R_j = 2(1 - c_s)$   $R_j = 2(1 - c_s)$  match the above movement of prey which changes with  $k$ ,  $c_s = rand(0,1)$ .

#### 2) Hard Besiege Mode

For  $e \geq 0.5$  and  $|E| < 0.5$ ,  $|E| < 0.5$ , the prey gets exhausted, does not have any more energy to escape, and gets surrounded by the hawks scarcely. The hawk's position is given in (7):

$$H(k+1) = H_{rabbit}(k) - E |\Delta H(k)| \quad (7)$$

#### 3) Soft Besiege with Rapid Dives

For  $e < 0.5$  and  $|E| \geq 0.5$ ,  $|E| \geq 0.5$ ,  $|E| \geq 0.5$ , the prey has adequate energy and squirts fruitfully. In this period, a Levy flight (LF) outline is employed to duplicate the crisscross perplexing attempt of prey and the rapid and hurried leap of hawks. The hawk's locations are written as:

$$H(k+1) = \begin{cases} S_b & \text{if } J(S_b) < J(H(k)) \\ S_{LF} & \text{if } J(S_{LF}) < J(H(k)) \end{cases} \quad (8)$$

Where  $J = \text{Objective Function}$

The hawks initially perform soft besiege, and if the result of this push is not improved, then pattern build plunge is completed as

$$S_b = H_{rabbit}(k) - E |R_j H_{rabbit}(k) - H_m(k)| \quad (9)$$

$$S_{LF} = S_b + V \times LF(d) \quad (10)$$

Where,  $d$ : variable's dimension,  $V$ : random vector with dimension  $1 \times d$ , and LF represents the LF function, which is given in (11) as follows:

$$LF(d) = 0.01 \times \frac{u \times \sigma}{|v|^{\frac{1}{\beta}}}, \sigma = \left[ \frac{\Gamma(1+\beta) \times \sin\left(\frac{\pi\beta}{2}\right)}{\Gamma\left(\frac{1+\beta}{2}\right) \times \beta \times 2^{\left(\frac{\beta-1}{2}\right)}} \right]^{\frac{1}{\beta}} \quad (11)$$

Where,  $u$  and  $v = rand(0,1)$  and  $\beta = 1.5$ .

#### 4) Hard Besiege Mode with Rapid Dives

For  $r < 0.5$  and  $|E| < 0.5$ , the prey's escaping energy has decreased appreciably. At this stage, hawks reduce their mean gap from the prey and execute a hard besiege. At this instant, the LF model is also used by hawks along with hard besiege to capture the prey successfully. This behavior of hawks is modeled in (12):

$$H(k+1) = \begin{cases} S_h & \text{if } J(S_h) < J(H(k)) \\ S_{LF} & \text{if } J(S_{LF}) < J(H(k)) \end{cases} \quad (12)$$

Where,  $S_h$  and  $S_{LF}$  are given in (13) and (14) as follows:

$$S_h = H_{rabbit}(k) - E |R_j H_{rabbit}(k) - H_m(k)| \quad (13)$$

$$S_{LF} = S_h + V \times LF(d) \quad (14)$$

In HHO [19], the switching from exploration to exploitation phase takes place based on the prey's escape energy value. Excessive exploration of the search area introduces randomness and may result in getting trapped in local minima. Furthermore, high exploitation introduces less randomness and optimum results may not be attained. Hence, an appropriate balance needs to be conserved between the exploration and exploitation phase during the search process. Also, in the current work,  $E$  and  $E_0$  are calculated by (15) and (16) contrary to (3) and (4) in HHO.

$$E = 2E_0 \left( 1 - \frac{k^{0.5}}{l^{0.5}} \right) \quad (15)$$

$$E_0 = 2 \cdot \cos(rand()) - 1 \quad (16)$$

It is evident from (15) that a lesser number of iterations is allocated for the exploration phase than the exploitation phase which is achieved by a cosine function used in (16). The cyclic cosine function relocates the solution which ensures suitable exploration of the search area and the method can be searched in another place and also between their equivalent locations.

In the HHO, the remaining hawks attempt to adjust their locations depending on the best location. In the beginning, the best location for hawks is unknown. As a result, the scheme of using initial big steps may affect moving whales away from the optimum value. Thus, SFs are engaged to control the movement of hawks in the initial phase. For all iterations, the location of hawks ( $H_m(k)$ ) is modified as given in (17):

$$H_m(k) = \frac{H(k)}{SF} \quad (17)$$

Where, SF is changed as given in (18):

$$SF = 2 - \frac{k}{l} \quad (18)$$

Insertion of SFs allows the hawks to shift gradually in the first phase of search progression thus recovering the searching ability of HHO. In the advanced phases, hawks move at a normal rate when better results are realized. The complexity remains the same in its implementation as the number of nested loops in the original HHO and

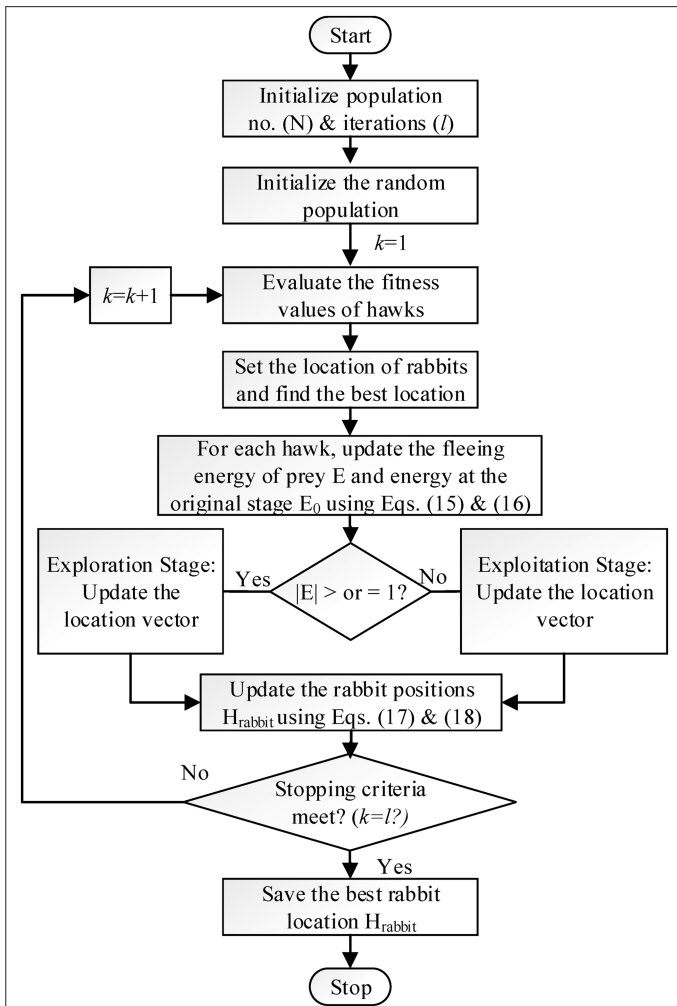


**Fig. 1.** Flowchart of EHHO algorithm. EHHO, enhanced Harris Hawks optimization.

EHHO is the same. The flowchart of the suggested EHHO is illustrated in Fig. 1.

### III. ENGINEERING DESIGN PROBLEM

#### A. Test System

The MGS considered in the recent study is a realistic system comprising of RESs, i.e., wind energy and solar PV. Since the randomness of RESs generation might lower the ratings of energy storage devices (ESDs) like fuel cell (FC), electric vehicle (EV), and ultracapacitor (UC) are included in the system to conquer the steadiness-linked problems. The FC and EV have greater time constants (TCs) than UC; hence, they respond quickly. Therefore, the general system dynamics are preserved by the comparative TCs and gain parameters of different elements. As the necessary dynamics have been incorporated, common inferences can be concluded from outcomes of real-time implementation. The schematic diagram and transfer function (TF) representation of the recommended MGS are specified in Figs 2 and 3, respectively. The structure data are specified in Appendix. The MGS comprises two wind turbine generators (WTGs), one PV, and two FCs.

For frequency studies, the dynamic systems can be represented by first-order TFs for PV, WTG, AE, FC, UC, and EV (19) – (24) with the related gain and TCs specified in Appendix. These TFs correspond to the electrical power produced ( $P_{WTG}$ ,  $P_{PV}$ ) by RESs. The AE makes hydrogen for the FC via a fraction of the power produced from the RESs. In the study, a centralized controller for the studied system is employed (Fig. 3) instead of many decentralized controllers for each subsystem. These aid in reducing wiring, easier preservation, and also formulate the planning problem easily by decreasing the number of controller parameters. But due to identical control signals employed in each subsystem, its performance may degrade. Even so, it is observed that the centralized scheme offers acceptable time-domain performance. In Fig. 2, UC and EV are controlled by T2FFOPID. They discharge or absorb energy to or from the grid in case of shortfall or excess power, correspondingly. As the dissimilar elements are situated at diverse locations, they are understood

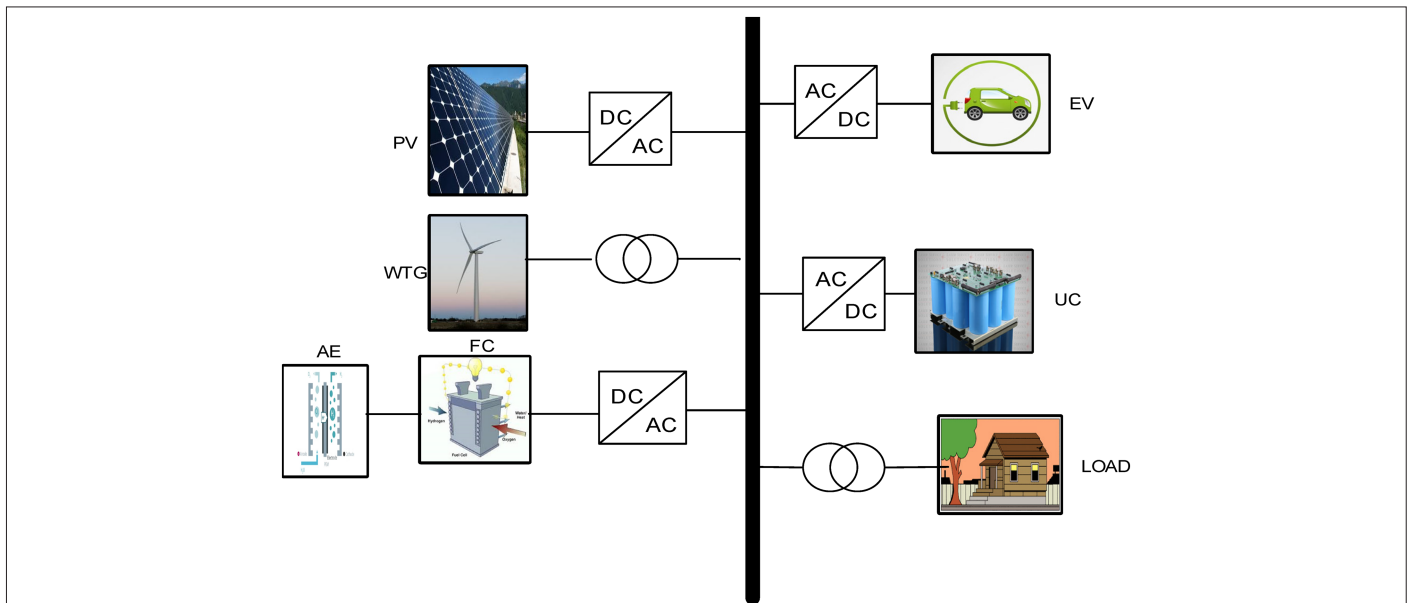


**Fig. 2.** Arrangement of the suggested AC microgrid.

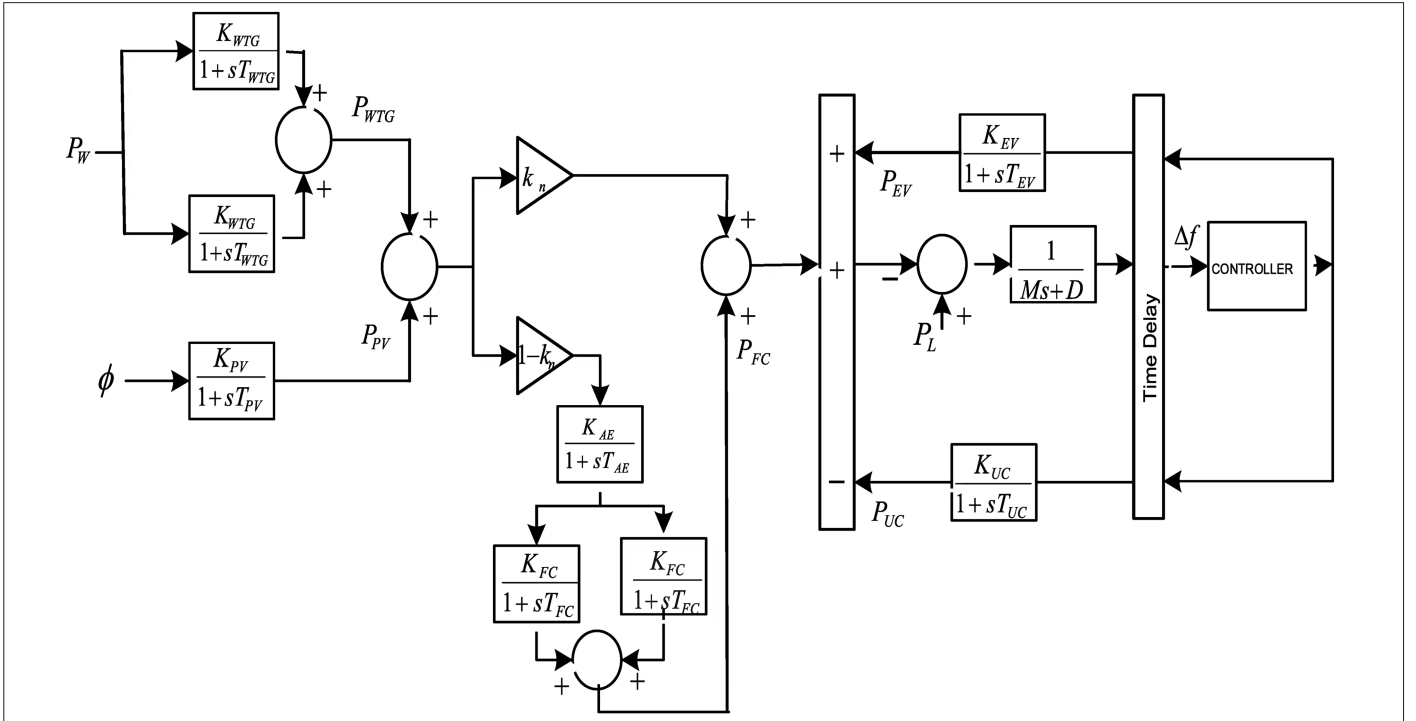


Fig. 3. Studied AC microgrid.

to converse through a common communication means which initiates time delays (TD) among the sensor to a controller to the actuator. Consequently, these TDs must be included in the design process.

### B. Modelling of Generating Units

Mathematical modeling of the solar PV, fuel cell, and WTG is carried out and its linear first-order transfer functions are given in (19-21) with associated gains ( $K_{PV}, K_{FC}, K_{WTG}$ ) and TCs ( $T_{PV}, T_{FC}, T_{WTG}$ ) presented in Appendix [2, 26] where  $n$  correspond to the number of units of each source.

$$G_{PV}(s) = \frac{K_{PV}}{1 + sT_{PV}} = \frac{\Delta P_{PV}}{\Delta \phi} \quad (19)$$

$$G_{FCn}(s) = \frac{K_{FC}}{1 + sT_{FC}} = \frac{\Delta P_{FC}}{\Delta P_{AE}} \quad n = 1, 2 \quad (20)$$

$$G_{WTGn}(s) = \frac{K_{WTG}}{1 + sT_{WTG}} = \frac{\Delta P_{WTG}}{\Delta P_W} \quad n = 1, 2 \quad (21)$$

AE uses  $(1 - k_n)$  part of the energy generated by RESs and liberates hydrogen as necessary by the FC given in (22) and  $k_n$  is chosen as 0.6 [1, 2].

$$G_{AE}(s) = \frac{K_{AE}}{1 + sT_{AE}} \quad (22)$$

The UC efficiently receives the excess energy from the RESs and supplies it to the load during decreased generation as given in (23)

$$G_{UC}(s) = \frac{K_{UC}}{1 + sT_{UC}} \quad (23)$$

EV aggregator comprises a fleet of EVs. The first-order transfer function of EV is given in (24) [27].

$$G_{EV}(s) = \frac{K_{EV}}{1 + sT_{EV}} \quad (24)$$

Where  $K_{EV}$  and  $T_{EV}$  are the gain and TC. The ESDs are provided with appropriate rate constraint non-linearity as shown in Fig. 4 to restrain the mechanical jerk. These are provided by  $|P_{UC}| < 1.2$   $|P_{EV}| < 0.15$ . This is a real situation as this will stop any ESDs to amass or discharge quickly. The power system is represented in (25)

$$G_{sys}(s) = \frac{\Delta f}{\Delta P_e} = \frac{\left(\frac{1}{D}\right)}{1 + s\left(\frac{M}{D}\right)} = \frac{K_p}{1 + sT_p}; \quad K_p = \left(\frac{1}{D}\right); \quad T_p = \left(\frac{M}{D}\right) \quad (25)$$

Where  $K_p$  and  $T_p$  represent the gain and time constant of the power system, respectively.  $D$  and  $M$  are the damping coefficient and mechanical inertia of the power system, respectively.

### C. Controller Configuration

The conventional FLC becomes ineffective in enhancing system performances when the system is subjected to considerable uncertainties [12]. In the current study, frequency control of MGS using a

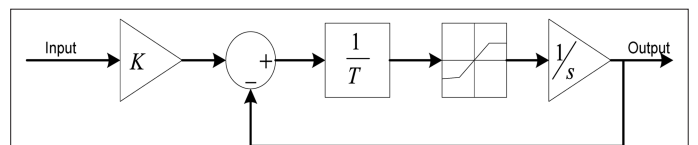


Fig. 4. Generation rate constraint (GRC) for energy storing element.

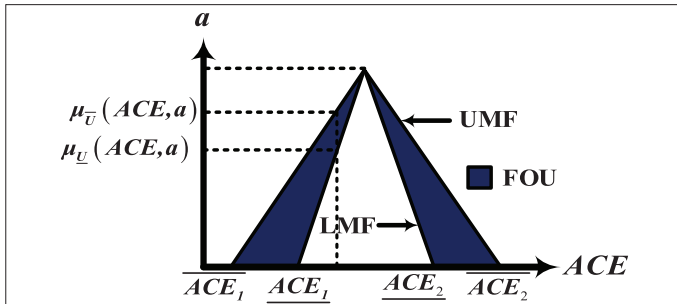


Fig. 5. Lower and upper membership functions [12].

T2FFOPID controller is suggested. The type-2 FLC, conjoining UMF and LMF, is shown in Fig. 5. A footprint of uncertainty (FOU) within the constraints is constructed among UMF and LMF. The input MFs  $(e \text{ and } \frac{de}{dt})$  are shown in Fig. 6. The FLC rule base and linguistic variables used for MFs are given in Table I. The T2 fuzzy set is articulated as given in (26):

$$FS = \{(Var, a), \mu_U(Var, a)\}, \forall Var \in P, \forall a \in J_{Var} [0, 1] \quad (26)$$

Where,  $\mu_U(Var, a)$  is the upper membership function,  $Var, a$  is the major and extra variable of the domain  $J_{Var}$  respectively.

The universe of discourse is given in (27):

$$FS = \int_{Var \in P} \int_{a \in J_{Var} [0, 1]} \frac{\mu_U(Var, a)}{(Var, a)} \quad (27)$$

Where  $\int \int =$  Union on ACE and  $a$

The expression can be given in (28):

$$\mu_U(Var, a) = \overline{FOU(U)} \forall Var \in P, \forall a \in J_{Var} [0, 1] \quad (28)$$

Where  $J_{Var}$  is given in (29):

$$J_{Var} = [\mu_U(Var, a), \mu_L(Var, a)] \forall Var \in P, \forall a \in J_{Var} [0, 1] \quad (29)$$

For type-2 FLC, the input signals are  $Var, dVar$  and the output is  $y$ . The structural attribute of the Type-2 FLC is given in (30-31)

$$LMF : \text{for } Var = \underline{LN}; dVar = \underline{Z}; Y = \underline{LN} \quad (30)$$

$$UMF : \text{for } Var = \overline{LN}; dVar = \overline{Z}; Y = \overline{LN} \quad (31)$$

The related fuzzy sets are given in (32-34)

$$\mu_U(Var, a) \quad (32)$$

$$\bar{f}^s = \max \{ \mu_{US}(Var, a), \mu_{US}(dVar, a) \} \quad (33)$$

$$FS = [ \underline{f}^s, \bar{f}^s ] \quad (34)$$

Type reducer is used to modify the fuzzy set from type-2 to type-1 for defuzzification. The center of sets (SOC) method is used for defuzzification. The outputs are given in (35-37):

$$Y_{cos} = \sum_{s=1}^{25} \frac{F^s Y^s}{F^s} = [Y_{m1}, Y_{m2}] \quad (35)$$

$$Y_{m1} = \frac{\sum_{s=1}^{25} f^s y^s}{\sum_{s=1}^{25} f^s} \quad (36)$$

$$Y_{m2} = \frac{\sum_{s=1}^{25} \bar{f}^s y^s}{\sum_{s=1}^{25} \bar{f}^s} \quad (37)$$

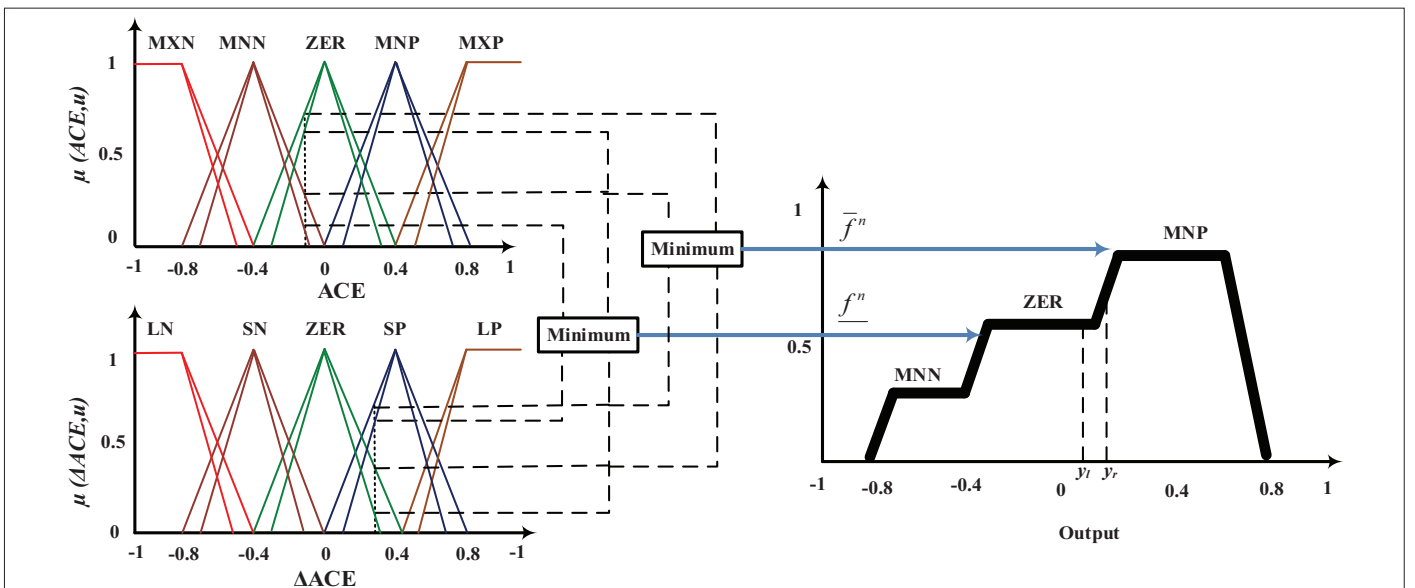


Fig. 6. Input and output membership functions [12].

**TABLE I.** FUZZY CONTROLLER RULE BASE

$e$	$\dot{e}$				
	EN	SN	ZER	SP	EP
EN	EN	EN	SN	SN	ZER
SN	EN	SN	EN	ZER	SP
ZER	SN	SN	ZER	SP	SP
SP	SN	ZER	SP	SP	EP
EP	ZER	SP	SP	EP	EP

SN: Small Negative; EN: Extreme negative; ZER: Zero; SP: Small Positive; EP: Extreme Positive.

Where,  $Y_{m1}$  and  $Y_{m2}$  are correlated to MFs of type-1 FLC. The proposed T2FFOPID implements the fractional order calculus and T2 FLC as demonstrated in Fig. 7.

**D. Objective Function**

In this optimization task, the proposed controller parameters are searched till the objective function ( $J$ ) attains the least value. In Integral Time Absolute Error (ITAE) and Integral Time Square Error (ITSE) measures, it weights errors occurring at the later stages since the error is multiplied by time. In Integral Absolute Error (IAE) measure, time is not multiplied but is likely to yield a sluggish response than Integral Square Error (ISE). However, ISE is the performance index that gives equal significance to frequency errors occurring all over the simulation time irrespective of their magnitude and occurrence time. Hence, in this study, ISE is chosen as the  $J$ . The general expression for the  $J$  is given in (38):

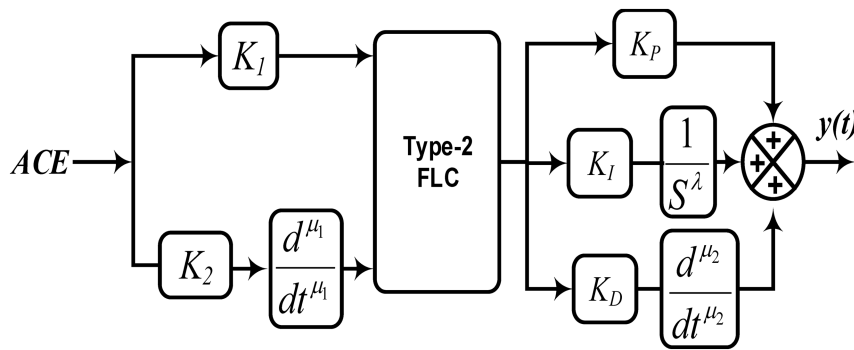


**Fig. 7.** Structure of T2FFOPID. T2FFOPID, type-2 fuzzy fractional order proportional integral derivative.

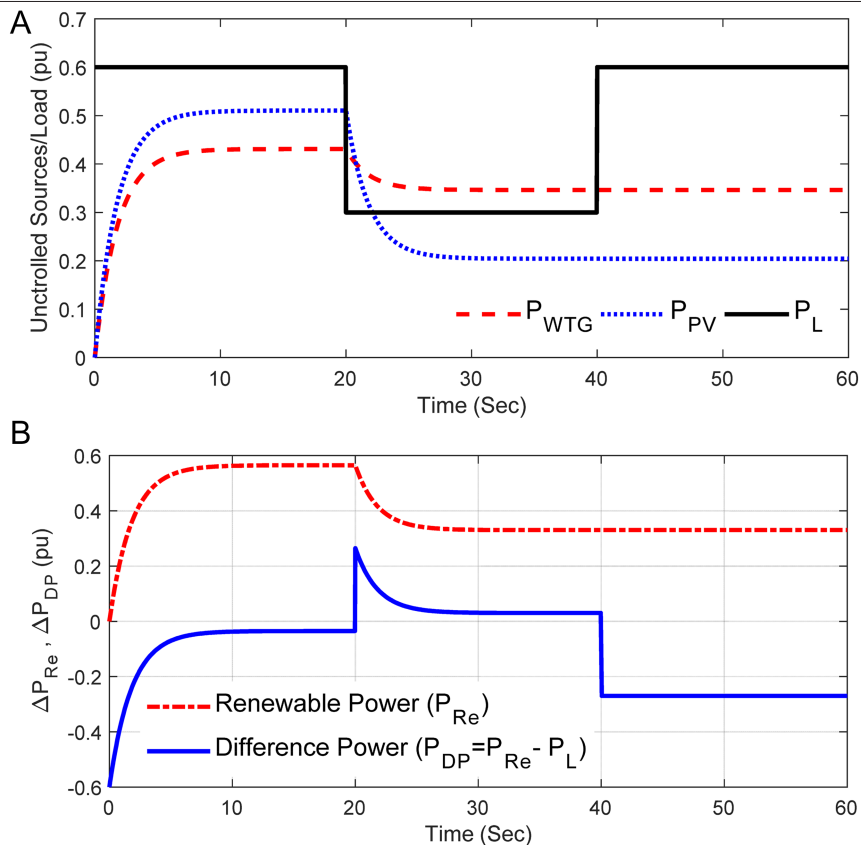


**Fig. 8.** (A). Uncontrolled sources and load of AC microgrid. (B). Total generation power and imbalance power of MG for case-1. MG, microgrid.

**TABLE II.** PARAMETERS OF COMPARED METHODS

Technique	Description	Parameter
GA	Tournament	Selection
	0.9 and 0.1	Crossover and mutation rates
PSO	Reduces from 0.9 to 0.2	Inertia weight, $w$
	2	Social & Cognitive components, $c_1$ & $c_2$
GSA	1, 20	Value of $G_0$ and Constant, $\alpha$
GWO	Reduces from 2 to 0	Parameter "a"
	Random number in range 0 to 1	Parameters $r_1, r_2$
HHO	2. rand ()-1	Energy at original stage, $E_0$
	$2E_0 \left(1 - \frac{k}{l}\right)$	Fleeing energy of prey, $E$
EHHO	2. cos (rand ())-1	Energy at original stage, $E_0$
	$2E_0 \left(1 - \frac{k^{0.5}}{l^{0.5}}\right) 2E_0 \left(1 - \frac{k^{0.5}}{l^{0.5}}\right)$	Fleeing energy of prey, $E$
	Reduces from 2 to 1	Scaling factor

GA, genetic algorithm; GSA, gravitational search algorithm; GWO, Grey wolf optimization; HHO, Harris hawks optimization; EHHO, enhanced Harris hawks optimization.

$$J = ISE = \int_0^{t_{sim}} \left[ k_n w (\Delta f)^2 + (1-w)(\Delta u)^2 \right]. dt \quad (38)$$

$t_{sim}$  is the simulation time.

The objective function includes two weighted parameters that aim to reduce frequency variation and control signal variation in the studied system. The parameter  $w$  defines the relative significance of the two objectives. In this study, equal weight is given to both elements of the control objective and hence  $w$  is set to 0.5.  $k_n$  is the normalizing constant to level the component of  $J$ . In (38), to formulate both the parts competitively during the search procedure,  $k_n$  is taken as 200.

#### IV. RESULTS

Subsequently, the effectiveness of the T2FFOPID controller tuned by the EHHO technique for frequency regulation of MGS is demonstrated in this study. The proposed MGS is modeled using MATLAB SIMULINK and the EHHO routine is formulated in a MATLAB code file. The SIMULINK model is run in a separate MATLAB code file with the first population assuming the variations in  $P_{WTG}$ ,  $P_{PV}$ , and  $P_L$ . The  $J$  value is found in the MATLAB code file and employed in the optimization technique. The load demand pattern and uncontrolled sources of an MGS are illustrated in Fig. 8(a). The entire power imbalance and renewable power of MGS are shown in Fig. 8(b). The frequency varies due to power disparity which is to be concealed by the suitable controller action. Different controller structures like PID, Fuzzy PID (FPID), and T2FFOPID are taken and the controller gain parameters are optimized by HHO and EHHO methods. The configuration of FPID is similar to T2FFOPID shown in Fig. 7; however, the FO derivatives/integers are substituted by

**TABLE III.** TUNED PARAMETERS

Technique/Controller	$K_1$	$K_2$	$\mu_1$	$K_p$	$K_i$	$K_D$	$\mu_2$	$\lambda$	J Value
AC Microgrid System									
GA/PID	–	–	–	1.5690	0.9897	1.8357	–	–	0.1579
PSO/PID	–	–	–	1.9549	1.9769	1.9949	–	–	0.1397
GSA/PID	–	–	–	1.8951	0.8857	1.9294	–	–	0.1327
GWO/PID	–	–	–	1.9431	1.2406	1.9949	–	–	0.1310
HHO/PID	–	–	–	1.9435	1.0302	1.9833	–	–	0.1297
EHHO/PID	–	–	–	1.9889	0.8826	1.9949	–	–	0.1269
EHHO/FPID	1.9847	1.9867	–	1.8959	1.9742	0.0081	–	–	0.0834
GA /T2FFOPID	1.4132	1.3441	0.7963	1.3392	1.1195	0.3499	0.5676	0.7639	0.0752
PSO /T2FFOPID	1.4631	1.1791	0.5690	1.8537	1.1768	0.2105	0.5062	0.7853	0.0671
GSA /T2FFOPID	1.4002	1.5507	0.4687	1.5096	1.2084	0.2389	0.5601	0.5850	0.0641
GWO /T2FFOPID	1.0458	1.3688	0.4055	1.5761	1.3970	0.2883	0.4584	.5555	0.0626
HHO /T2FFOPID	1.0979	1.5954	0.8011	1.4315	1.3671	0.4987	0.7472	.3852	0.0609
EHHO/T2FFOPID	1.1148	1.4466	0.8655	0.8993	1.9844	1.3502	0.1063	.9316	0.0586

GA, genetic algorithm; GSA, gravitational search algorithm; GWO, Grey wolf optimization; HHO, Harris hawks optimization; EHHO, enhanced Harris hawks optimization; PID, proportional integral derivative; T2FFOPID, type-2 fuzzy fractional order proportional integral derivative.

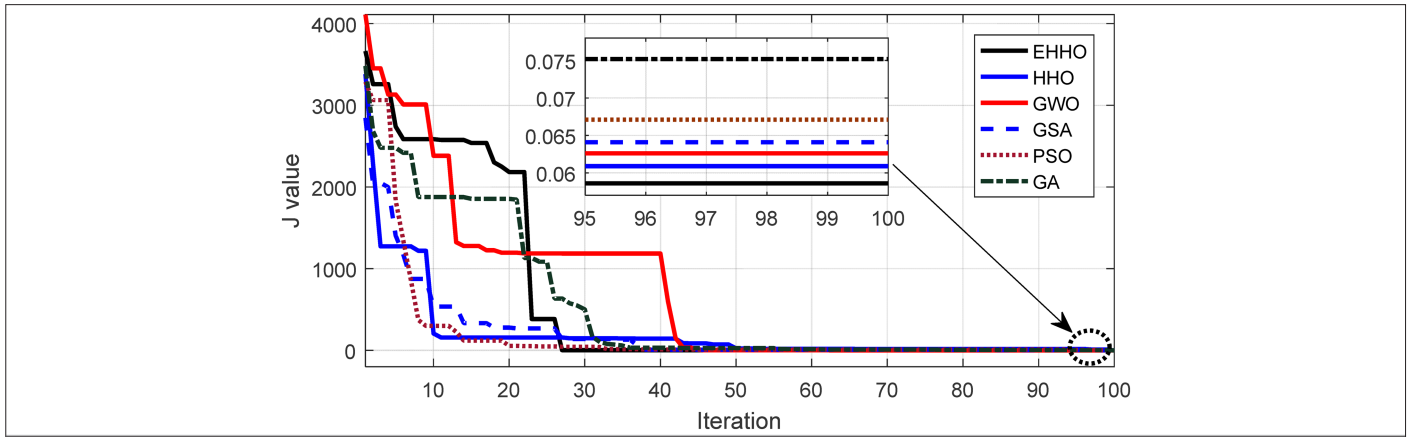


**Fig. 9.** Comparison of convergence curves with different algorithms.

integer-ordered counterparts and T2 FLC is substituted by corresponding type 1. The outcomes of the proposed scheme are also compared with a few current methods like PSO, GA, GSA, and

GWO. All the parameters used for different algorithms are given in Table II. The number of function evaluations carried out is 3000 for every technique to formulate a reasonable assessment. In all

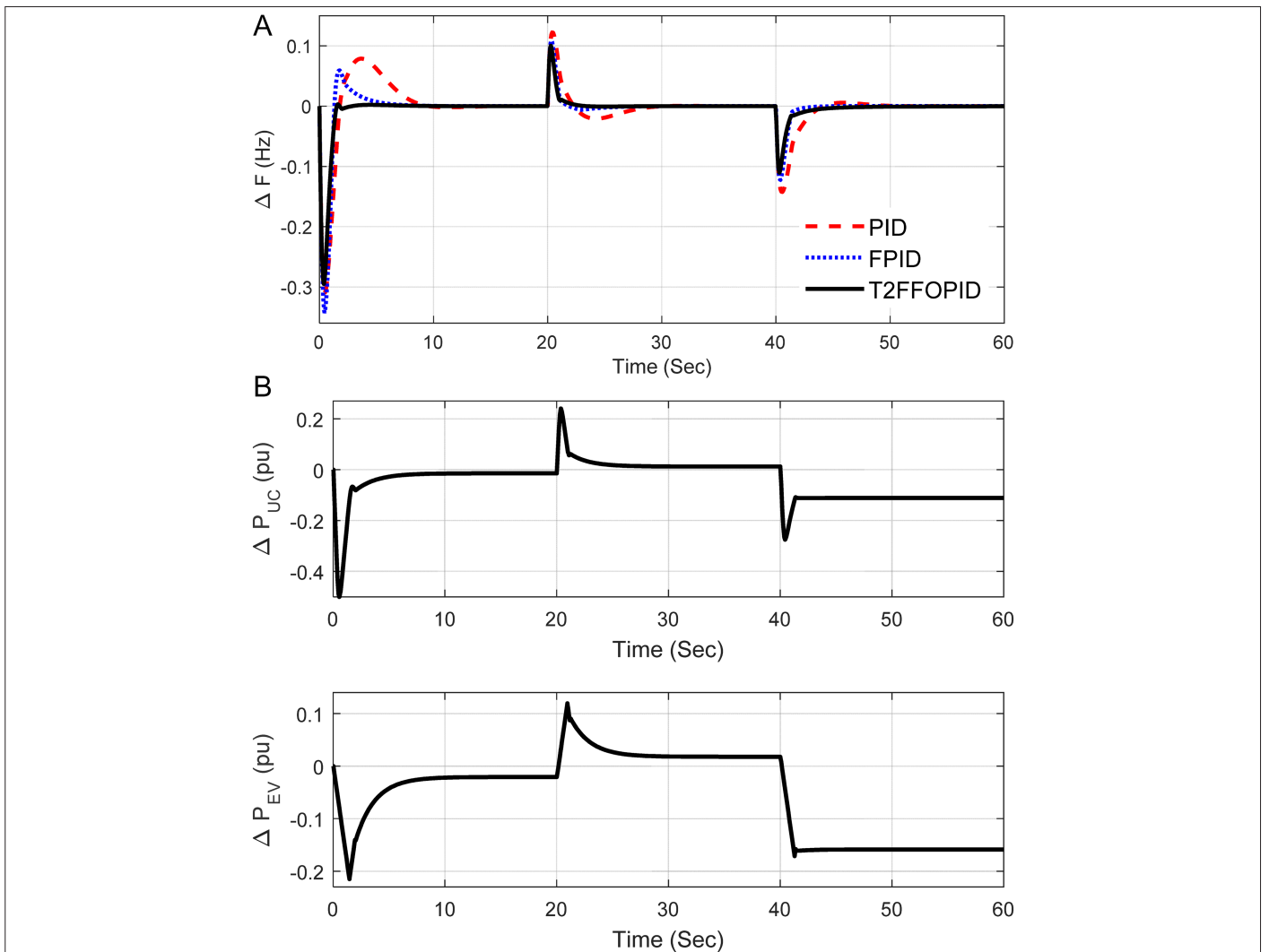


**Fig. 10.** (A).  $\Delta F$  response for case-1. (B). Controllable sources with T2FFOPID for case-1. T2FFOPID, type-2 fuzzy fractional order proportional integral derivative.

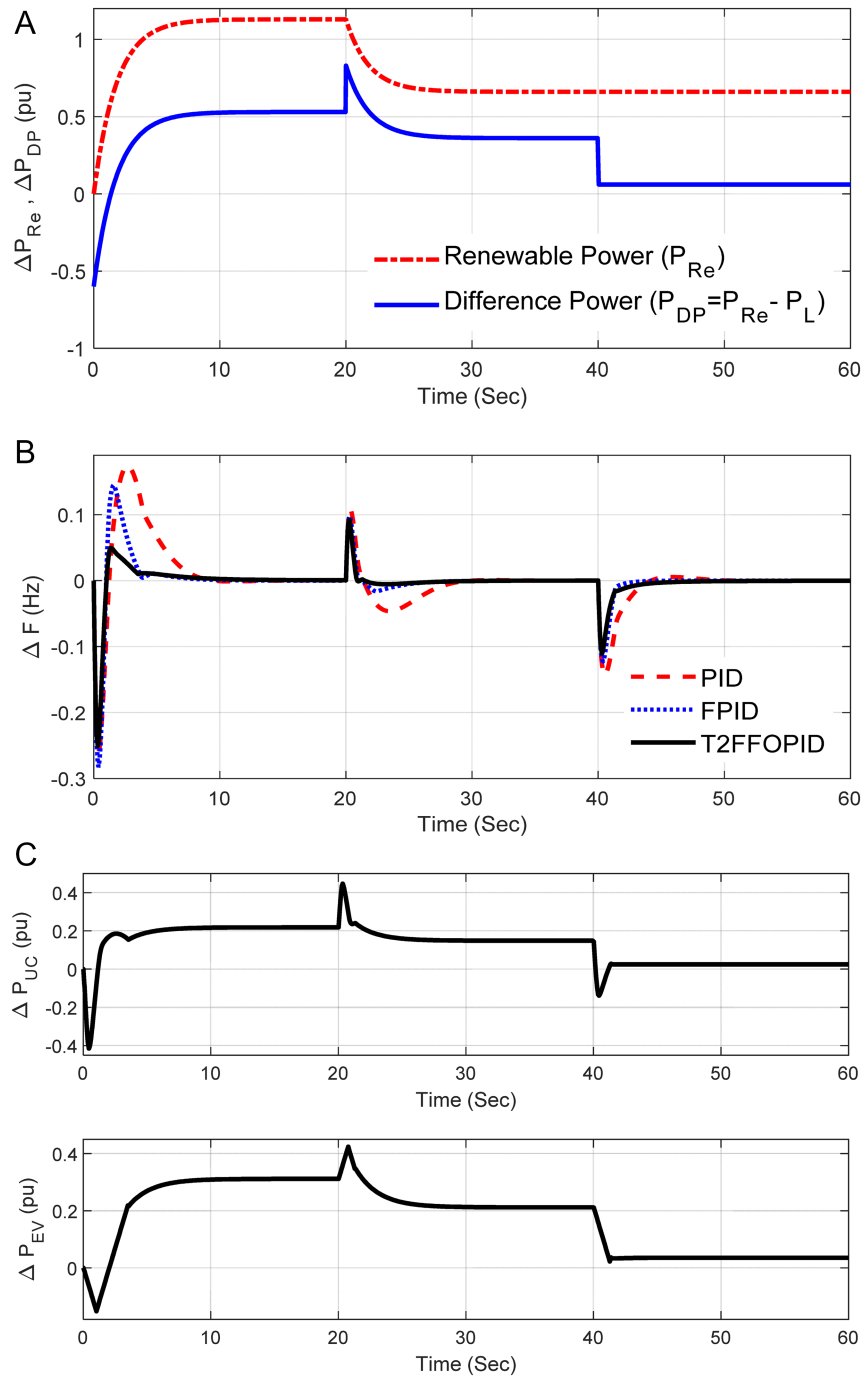


**Fig. 11.** (A). The total power and imbalance power of MGS for case-2. (B).  $\Delta F$  response for case-2. (C). Instantaneous power for case-2. MGS, microgrid system.

the algorithms, 100 iterations were carried out using 30 search agents.

The gain parameters for PID, FPID, and T2FFOPID controller are selected in the range of  $-2, 2$ . All the proposed approaches are performed in 20 epochs, and the best results with the least  $J$  value are used as optimal parameters. The tuned parameters are given in Table III. From Table III, it can be observed that PID controller with HHO ( $J = 0.1297$ ) as compared to GA ( $J = 0.1579$ ), PSO ( $J = 0.1397$ ), GSA ( $J = 0.1327$ ), and GWO ( $J = 0.1310$ ). The  $J$  cost is further reduced

to 0.1269 when optimized by EHHO. For PID controller tuning, a percent decrement in  $J$  with the proposed EHHO method is better than other competing techniques. The convergence graphs given in Fig. 9 confirm that EHHO outperforms other competing techniques. The  $J$  values are further reduced while FPID and T2FFOPID are used and the least  $J$  ( $J = 0.0586$ ) is obtained with EHHO-based T2FFOPID. To demonstrate the performance of EHHO-based T2FFOPID, different case studies are considered. The performance of all other studied algorithms is also compared with EHHO for tuning T2FFOPID, and the results are presented in Table III. The percent reduction in  $J$  with

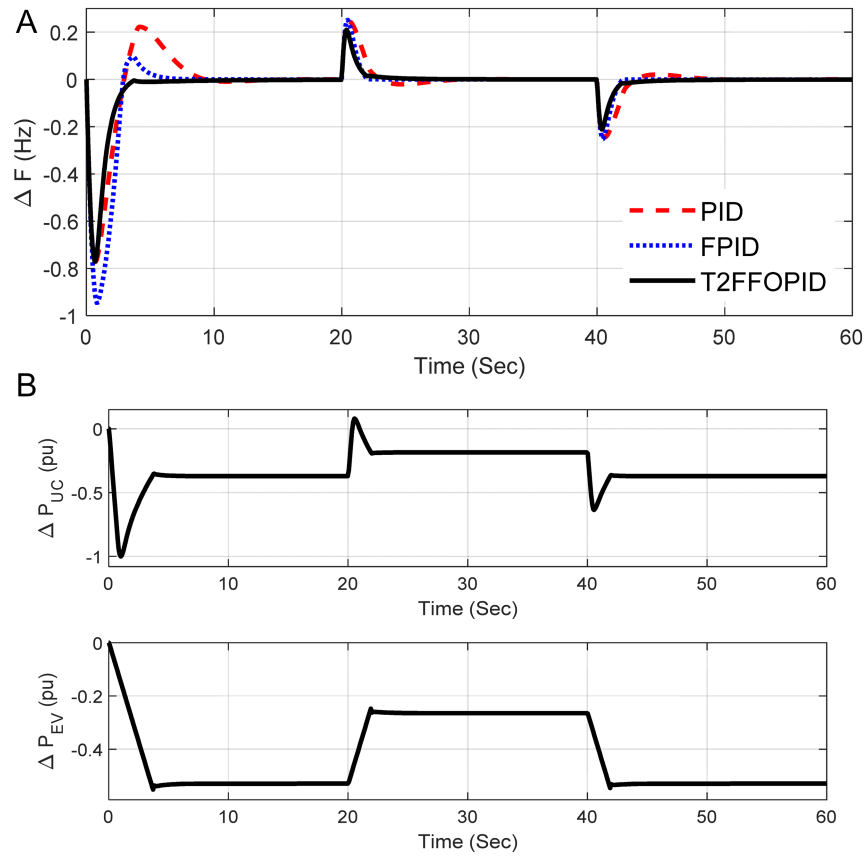


**Fig. 12.** (A).  $\Delta F$  response for case-3. (B). Instantaneous power for case-3.

**TABLE IV.** EVALUATION OF EHHO-TUNED CONTROLLERS

Controller/Performance	Integral Errors				Overshoots (O <sub>i</sub> )	Undershoots (U <sub>i</sub> ) (-ve)
	ISE	ITAE	IAE	ITSE		
Case-1: Normal Operation						
PID	0.1269	16.2831	1.0837	1.2157	0.1225	0.3092
FPID	0.0902	6.8471	0.5787	0.5349	0.1088	0.3426
T2FFOPID	0.0586	6.8454	0.5787	0.5349	0.1001	0.2948
Case 2: Increased Renewable Power						
PID	0.13704	18.3404	1.2565	1.3440	0.1734	0.2591
FPID	0.0740	7.3482	0.6292	0.5168	0.1445	0.2824
T2FFOPID	0.0402	7.2785	0.6291	0.5162	0.0922	0.2501
Case 3: Unavailability of Renewable Power						
PID	0.9551	33.6808	2.8564	5.5037	0.2455	0.7718
FPID	1.3221	17.7458	2.3236	4.1292	0.2522	0.9467
T2FFOPID	0.5970	17.3725	2.3236	4.1292	0.2098	0.7707

EHHO, enhanced Harris hawks optimization; FPID, fuzzy proportional integral derivative; PID, proportional integral derivative; T2FFOPID, type-2 fuzzy fractional order proportional integral derivative.

**TABLE V.** UNCERTAINTY ANALYSIS

System Parameter	Perturbation	Integral errors				Overshoots ( $O_s$ )	Undershoots ( $U_s$ ) (-ve)
		ISE	ITAE	IAE	ITSE		
Model uncertainties	Nominal	.0586	6.8454	.5787	.5349	.1001	.2948
	Increase 25%	.0546	6.1296	.4115	.3368	.0989	.2938
	Decrease 25%	.0674	8.3970	.5191	.4596	.1022	.2970

the proposed EHHO-tuned T2FFOPID controller is the best as compared to other competing approaches.

**A. Case Study-1: Normal Operation**

In this case, wind energy generation and solar PV with demand load patterns as specified in Fig. 8 (a) are considered. The performance of PID, FPID, and T2FFOPID controller structures tuned by the proposed EHHO method is given in Fig. 10(a). The response with the proposed T2FFOPID controller structure is better than PID and FPID. The powers of controllable elements are shown in Fig. 10(b). It can be noticed from Fig. 8(b) that, during the negative power imbalance period (up to 20s), controllable elements provide the remaining power to reduce the power disparity. During a positive power imbalance period (20s–40s), i.e., when the load is less than the generation, controllable elements receive power from the Alternating Current (AC) MG to lessen the power inequity. During a higher negative power imbalance period (40s–60s), the controllable elements deliver more power. This demonstrates the superior capability of T2FFOPID controller over the PID and FPID controllers. The improved results are realized with T2FFOPID due to its capability to deal with nonlinearity, thus achieving fast response and required control action.

**B. Case Study-2: Increased Contribution of Renewable Energy Source**

In this case, solar PV and wind energy generation are amplified by 100%. The instantaneous RES power and the different power of MGS are displayed in Fig. 11(a). From Fig. 11(b), it can be noticed that the response of T2FFOPID is superior to PID and FPID. The powers of

controllable elements are illustrated in Fig. 11(c). As seen in Fig. 11(a), the RES generation is higher than the load so the input power of the regulated elements is positive. Depending on the magnitude of power inequity, the extent of power is provided by the regulated elements, i.e., the larger the power disparity, the higher the energy received by controlled elements.

**C. Case Study-3: Unavailability of Renewable Energy Source**

In this case, wind energy generation and solar PV are made unavailable and the pattern of load demand is amplified by 50%. Consequently, the entire renewable power generations are zero and demand is at all times higher than a generation. The outcome of this case is revealed in Fig. 12(a) and the powers of controllable elements are shown in Fig. 12(b). As the RES is less than the demand, the regulated elements supply energy to the MG. The performance of EHHO-based controllers is shown in Table IV where it can be seen that the recommended T2FFOPID outperforms as compared to PID and FPID controllers.

**D. Case Study-4: Uncertainty Analysis**

An uncertainty analysis is carried out; under larger changes in system parameters to verify the efficiency of the suggested EHHO-based T2FFOPID controller structure. The gains and time constants of PV, WTG, UC, EV, FC, and AE are simultaneously varied in the range from –25% to +25% and the outcomes are shown in Table V. It is perceived that the proposed approach is vigorous and performance indices remain nearly steady under simultaneously varied conditions.

The above cases confirm that the T2FFOPID controller can deal with increased/unavailability RES and uncertainties in system parameters in a better way than PID and FPID controllers.

**V. EVALUATION OF CURRENT FREQUENCY CONTROL SYSTEM**

The reliability of the proposed T2FFOPID tuned by EHHO is also examined in two equal-area interconnected power systems [28-31]. Two equal configurations of the T2FFOPID controller structure are assumed for each area due to their equal character. A step load disturbance (SLD) of +10% is applied at  $t=0$  second in area-1. The EHHO-tuned T2FFOPID controller gain parameters are found to be  $K_1$  (1.7117);  $K_2$  (1.9488);  $K_p$  (-0.2036);  $K_i$  (-1.3709);  $K_D$  (-0.5181);  $\lambda$  (0.8623);  $\mu_1$  (0.1342); and  $\mu_2$  (0.6848). The outcome of the proposed scheme is also compared with several other schemes like Ziegler Nichols (ZN) [28], Genetic Algorithm Proportional Integral (GA PI) [28], Bacterial Foraging Optimization Algorithm Proportional Integral (BFOA PI) [28], Differential Evolution Proportional Integral (DE PI) [29], PSO PI [30], hybrid BFOA-PSO PI [30], as well as Firefly Algorithm Proportional Integral (FA PI) PID controllers [31]. Table VI provides the performance index value from which it can be noticed that the least error criteria are achieved by EHHO-tuned T2FFOPID than some lately suggested AGC methods. The percentage reduction in ITAE

**TABLE VI.** COMPARISON WITH DIFFERENT METHODS FOR NON-REHEAT SYSTEM

Optimization method/ Controller	ITAE
Conv. ZN/ PI [28]	3.5768
GA/ PI [28]	2.7475
BFOA/ PI [28]	1.8379
PSO/ PI [30]	1.2142
hBFOA-PSO/ PI [30]	1.1865
DE/ PI [29]	0.9911
FA/ PI [31]	0.8695
FA/ PID [31]	0.4714
Proposed EHHO/T2FFOPID	0.2194

ZN, Ziegler Nichols; T2FFOPID, type-2 fuzzy fractional order proportional integral derivative; EHHO, enhanced Harris hawks optimization.

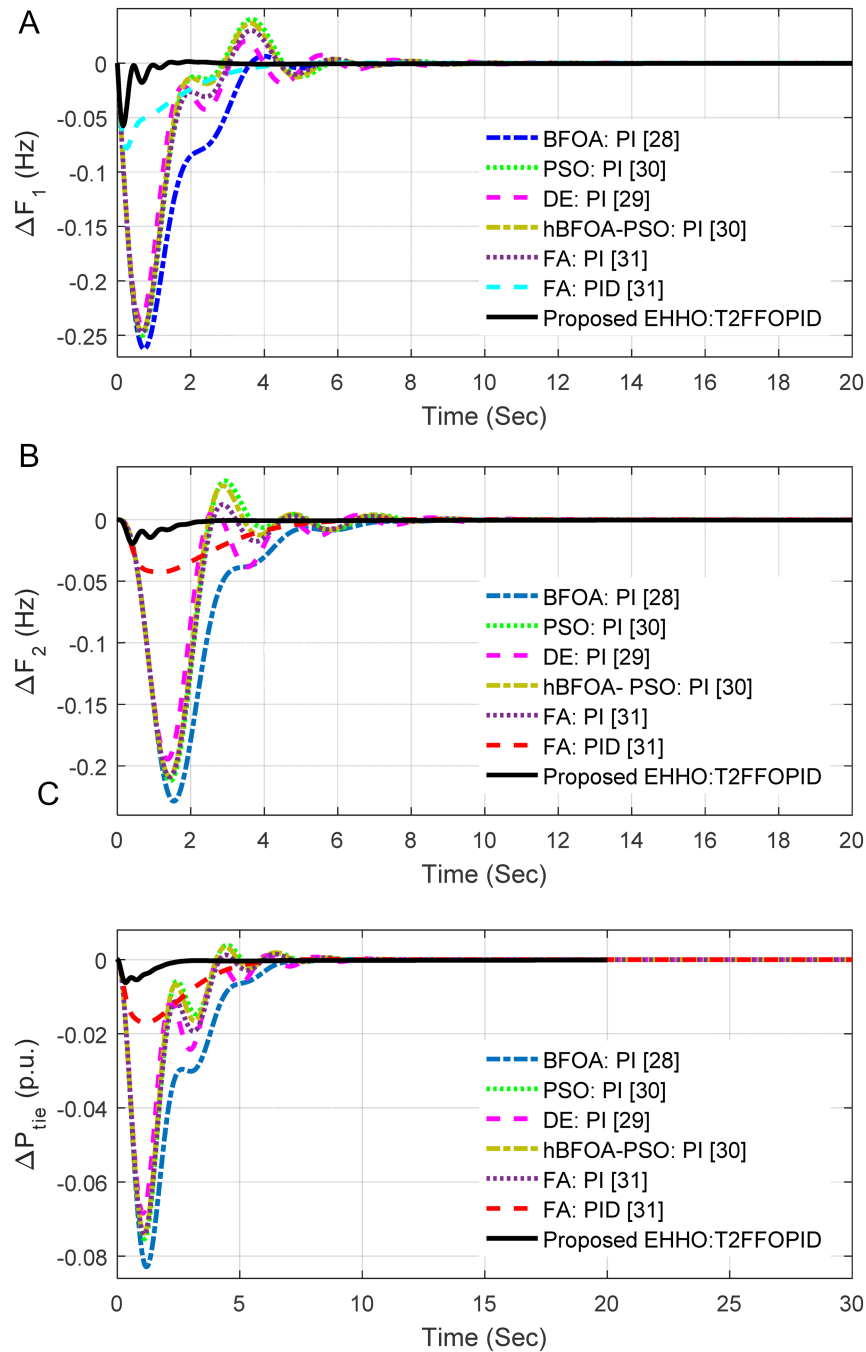


**Fig. 13.** Comparative response for two area non-reheat thermal power system (A)  $\Delta F_1$ , (B)  $\Delta F_2$ , (C)  $\Delta P_{tie}$ .

value as compared to the best available results (i.e., FA PID) is found to be 53.46%. The response for the same is given in Fig. 13(a)-(c), which displays that the EHHO-tuned T2FFOPID outperforms recently proposed AGC methods.

The proposed frequency control scheme is also applied to a widely used two-equal-area reheat thermal power system [32, 33, 34]. A SLD of +1% is assumed at  $t=0$  second in area -1. For this model, the EHHO-tuned T2FFOPID parameters are found to be  $K_1$  (1.8099);  $K_2$  (1.0314);  $K_p$  (-1.3262);  $K_I$  (-1.9011);  $K_D$  (-0.3207);  $\lambda$  (0.9194);  $\mu_1$  (0.9408); and  $\mu_2$  (0.3024). The performance was compared with PID

controllers tuned by Firefly algorithm (FA) [32], symbiotic organism search algorithm (SOSA) [33], and ABC [34]. It is noticed that least ITAE value ( $ITAE=0.71 \times 10^{-2}$ ) is attained with proposed EHHO-based T2FFOPID compared to FA PID [32] ( $ITAE=10.12 \times 10^{-2}$ ), SOSA PID [33] ( $ITAE=9.96 \times 10^{-2}$ ) and Artificial bee colony (ABC) PID [34] ( $ITAE=5.72 \times 10^{-2}$ ) for a two equal-area reheat thermal power system. The percentage reduction in ITAE value as compared to the best available results (i.e., ABC PID [34]) is found to be 87.58%. The response for the same is given in Fig. 14(a)-(c), which displays that the EHHO-tuned T2FFOPID outperforms recently proposed automatic generation control methods.

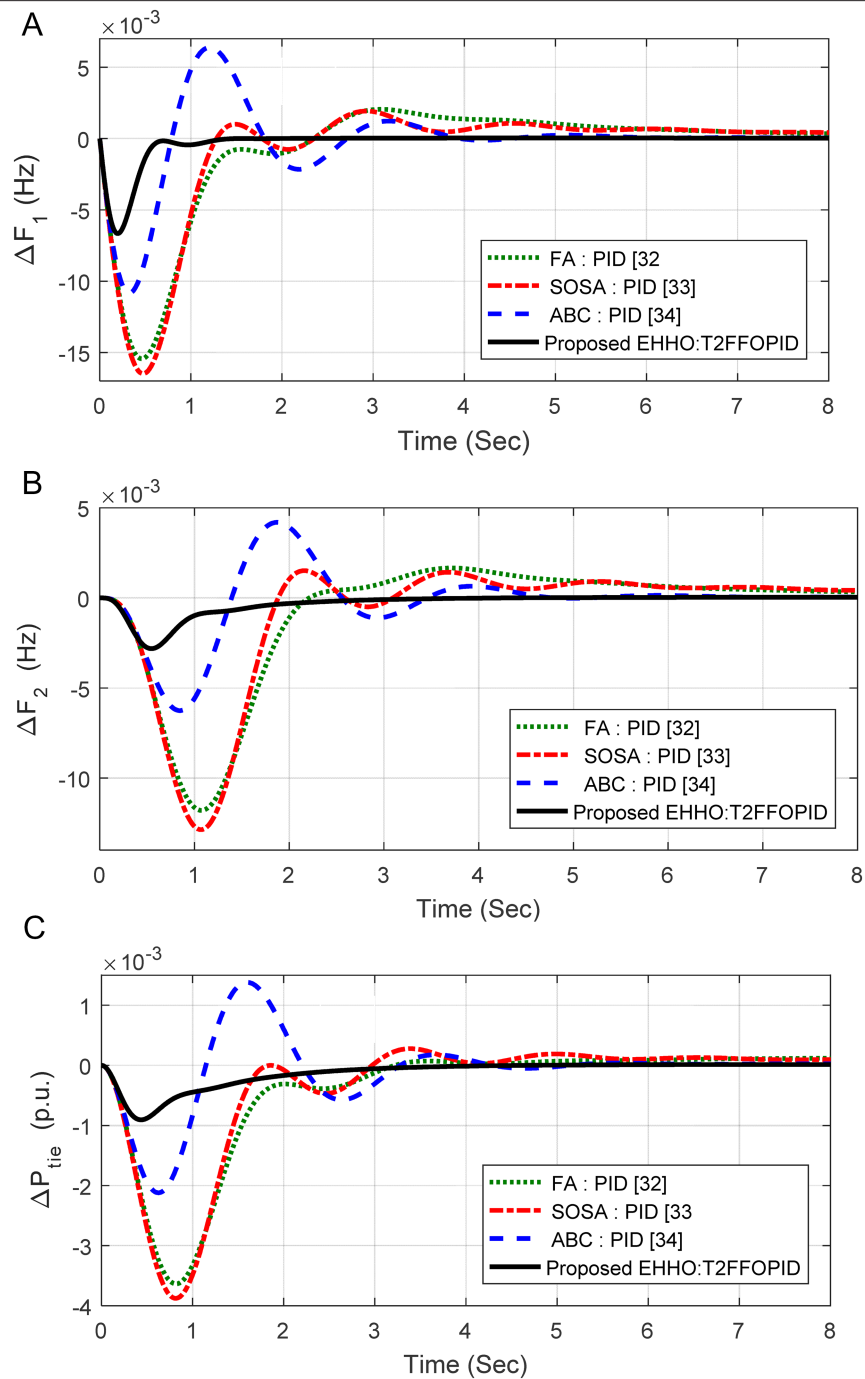


**Fig. 14.** Comparative response for two area reheat thermal power system (A)  $\Delta F_1$ , (B)  $\Delta F_2$ , (C)  $\Delta P_{tie}$ .

## VI. CONCLUSION

A comparative study for frequency control of MGS-containing several renewable energies and storage elements with EVs is presented in this work. A T2FFOPID controller structure is suggested for frequency control. The controller gain parameters are optimized by the EHHO method. It is noticed that the EHHO method outperforms the other competitive methods like HHO, PSO, GA, GSA, and GWO. The percent improvement in objective function by the proposed EHHO technique is better than the other methods. The performance of the T2FFOPID controller structure is compared

with PID and FPID under normal and anticipated operational conditions like bigger contribution and disconnection of RESs. It is noticed that the percent decrease in objective function with the suggested T2FFOPID controller as compared to PID and FPID is 53.82% and 29.74%, respectively. Further, significantly smaller amounts of errors, undershoots, and overshoots are acquired with the proposed T2FFOPID controller structure as compared to PID and FPID controllers. Also, there is a reduction in objective function values with the suggested frequency control method as compared to FA PID (53.46%) and ABC PID (87.58%) for the benchmark system.

**Peer-review:** Externally peer-reviewed.

**Author Contributions:** Concept – G.S., S.P.; Design – R.K.S., P.C.P.; Supervision – R.K.S., S.P.; Materials – G.S., P.C.P.; Data Collection and/or Processing – G.S., P.C.P.; Analysis and/or Interpretation – R.K.S., S.P.; Literature Review – G.S., P.C.P.; Writing – G.S., P.C.P.; Critical Review – R.K.S., S.P.

**Declaration of Interests:** The authors have no conflicts of interest to declare.

**Funding:** The authors declared that this study has received no financial support.

## REFERENCES

1. I. Pan, and S. Das, "Fractional order fuzzy control of hybrid power system with renewable generation using chaotic PSO," *ISA Trans.*, vol. 62, pp. 19–29, 2016. [\[CrossRef\]](#)
2. I. Pan, and S. Das, "Kriging based surrogate modeling for fractional order control of microgrids," *IEEE Trans. Smart Grid*, vol. 6, no. 1, pp. 36–44, 2015. [\[CrossRef\]](#)
3. P. Ray, S. Mohanty, and N. Kishor, "Small-signal analysis of autonomous hybrid distributed generation systems in presence of ultra capacitor and tie-line operation," *J. Electr. Eng.*, vol. 61, no. 4, pp. 205–214, 2010. [\[CrossRef\]](#)
4. R. K. Sahu, S. Panda, and G. T. C. Sekhar, "A novel hybrid PSO-PS optimized fuzzy PI controller for AGC in multi area interconnected power systems," *Int. J. Electr. Power Energy Syst.*, vol. 64, pp. 880–893, 2015.
5. Y. Arya, "Improvement in automatic generation control of two- area electric power systems via a new fuzzy aided optimal PIDN- FOI controller," *ISA Trans.*, vol. 80, pp. 475–490, 2018. [\[CrossRef\]](#)
6. M. H. Khooban, T. Dragicevic, F. Blaabjerg, and M. Delimar, "Shipboard microgrids: A novel approach to load frequency control," *IEEE Trans. Sustain. Energy*, vol. 9, no. 2, pp. 843–852, 2017. [\[CrossRef\]](#)
7. M. H. Khooban, T. Niknam, F. Blaabjerg, and T. Dragicevic, "A new load frequency control strategy for micro-grids with considering electrical vehicles," *Elect. Power Syst. Res.*, vol. 143, pp. 585–598, 2017. [\[CrossRef\]](#)
8. M. H. Khooban, T. Niknam, M. Shasadeghi, T. Dragicevic, and F. Blaabjerg, "Load frequency control in microgrids based on a stochastic noninteger controller," *IEEE Trans. Sustain. Energy*, vol. 9, no. 2, pp. 853–861, 2017. [\[CrossRef\]](#)
9. M. Gheisarnjad, and M. H. Khooban, "Secondary load frequency control for multi-microgrids: HiL real-time simulation," *Soft Comput.*, vol. 23, no. 14, pp. 5785–5798, 2019. [\[CrossRef\]](#)
10. P. K. Mohanty, B. K. Sahu, T. K. Pati, S. Panda, and S. K. Kar, "Design and analysis of fuzzy PID controller with derivative filter for AGC in multi-area interconnected power system," *IET Gener. Transm. Distrib.*, vol. 10, no. 15, pp. 3764–3776, 2016. [\[CrossRef\]](#)
11. A. Fereidouni, M. A. Masoum, and M. Moghbel, "A new adaptive configuration of PID type fuzzy logic controller," *ISA Trans.*, vol. 56, pp. 222–240, 2015. [\[CrossRef\]](#)
12. P. C. Sahu, S. Mishra, R. C. Prusty, and S. Panda, "Improved-salp swarm optimized type-II fuzzy controller in load frequency control of multi area islanded AC microgrid," *Sustain. Energy Grids Netw.*, vol. 16, pp. 380–392, 2018. [\[CrossRef\]](#)
13. G. Xiong, J. Zhang, D. Shi, and Y. He, "Parameter extraction of solar photovoltaic models using an improved whale optimization algorithm," *Energies*, vol. 174, pp. 388–405, 2019.
14. B. P. Sahoo, and S. Panda, "Improved grey wolf optimization technique for fuzzy aided PID controller design for power system frequency control," *Sustain. Energy Grids Netw.*, vol. 16, pp. 278–299, 2018. [\[CrossRef\]](#)
15. S. Arora, and P. Anand, "Binary butterfly optimization approaches for feature selection," *Expert Syst. Appl.*, vol. 116, pp. 147–160, 2019. [\[CrossRef\]](#)
16. M. M. Mafarja, and S. Mirjalili, "Hybrid Whale Optimization Algorithm with simulated annealing for feature selection," *Neurocomputing*, vol. 260, pp. 302–312, 2017. [\[CrossRef\]](#)
17. R. K. Khadanga, and A. Kumar, "Hybrid adaptive 'gbest'-guided gravitational search and pattern search algorithm for automatic generation control of multi-area power system," *IET Gener. Transm. Distrib.*, vol. 11, no. 13, pp. 3257–3267, 2017. [\[CrossRef\]](#)
18. N. Saha, and S. Panda, "Cosine adapted modified whale optimization algorithm for control of switched reluctance motor," *Comp. Intell.*, vol. 38, no. 3, pp. 978–1017, 2022. [\[CrossRef\]](#)
19. A. A. Heidari, S. Mirjalili, H. Faris, I. Aljarah, M. Mafarja, and H. Chen, "Harris hawks optimization: Algorithm and applications," *Future Gener. Comput. Syst.*, vol. 97, pp. 849–872, 2019. [\[CrossRef\]](#)
20. S. Khalilpourazary, and S. Khalilpourazary, "An efficient hybrid algorithm based on water cycle and moth-flame optimization algorithms for solving numerical and constrained engineering optimization problems," *Soft Comput.*, vol. 23, no. 5, pp. 1699–1722, 2019. [\[CrossRef\]](#)
21. S. Ekinici, D. Izci, and B. Hekimoğlu, "PID speed control of DC motor using Harris hawks optimization algorithm," in Proc. of the 2nd International Conference on Electrical, Communication and Computer Engineering (ICEECE), Istanbul, Turkey, 2020, pp. 1–6.
22. D. Izci, S. Ekinici, A. Demirören, and J. Hedley, "HHO algorithm based PID controller design for aircraft pitch angle control system," in International Congress on Human-Computer Interaction, Optimization and Robotic Applications (HORA), Ankara, Turkey, 2020, pp. 1–6.
23. D. Izci, and S. Ekinici, "An efficient FOPID controller design for vehicle cruise control system using HHO algorithm," in 3rd International Congress on Human-Computer Interaction, Optimization and Robotic Applications (HORA), Ankara, Turkey, 2021, pp. 1–6.
24. E. Eker, M. Kayri, S. Ekinici, and D. Izci, "Training multi-layer Perceptron using harris hawks optimization," in International Congress on Human-Computer Interaction, Optimization and Robotic Applications (HORA), Ankara, Turkey, 2020, pp. 1–5.
25. S. K. Govindaraju, and R. Sivalingam, "Design, analysis, and real-time validation of type-2 fractional order fuzzy controller for energy storage-based microgrid frequency regulation," *Int. Trans. Electr. Energy Syst.*, 2020. [\[CrossRef\]](#)
26. I. Pan, and S. Das, "Fractional order AGC for distributed energy resources using robust optimization," *IEEE Trans. Smart Grid*, vol. 7, no. 5, pp. 2175–2186, 2016. [\[CrossRef\]](#)
27. K. S. Ko, and D. K. Sung, "The effect of EV aggregators with time-varying delays on the stability of a load frequency control system," *IEEE Trans. Power Syst.*, vol. 33, no. 1, pp. 669–680, 2017. [\[CrossRef\]](#)
28. E. S. Ali, and S. M. Abd-Elazim, "Bacteria foraging optimization algorithm based load frequency controller for interconnected power system," *Int. J. Electr. Power Energy Syst.*, vol. 33, no. 3, pp. 633–638, 2011. [\[CrossRef\]](#)
29. U. K. Rout, R. K. Sahu, and S. Panda, "Design and analysis of differential evolution algorithm based automatic generation control for interconnected power system," *Ain Shams Eng. J.*, vol. 4, no. 3, pp. 409–421, 2013. [\[CrossRef\]](#)
30. S. Panda, B. Mohanthy, and P. K. Hota, "Hybrid BFOA-PSO algorithm for automatic generation control of linear and nonlinear interconnected power systems," *Appl. Soft Comput.*, vol. 13, no. 12, pp. 4718–4730, 2013. [\[CrossRef\]](#)
31. S. Padhan, R. K. Sahu, and S. Panda, "Application of firefly algorithm for load frequency control of multi-area interconnected power system," *Electr. Power Compon. Syst.*, vol. 42, no. 13, pp. 1419–1430, 2014. [\[CrossRef\]](#)
32. T. S. Gorripotu, R. K. Sahu, and S. Panda, "Comparative performance analysis of classical controllers in LFC using FA technique," in IEEE International Conference on Electrical, Electronics, Signals, Communication Optimization (EESCO): Visakhapatnam, Andhra Pradesh, India; 2015, pp. 1–5.
33. D. Guha, P. K. Roy, and S. Banerjee, "Symbiotic organism search algorithm applied to load frequency control of multi-area power system," *Energy Syst.*, vol. 9, no. 2, pp. 439–468, 2018. [\[CrossRef\]](#)
34. H. Gozde, M. Cengiz Taplamacioglu, and İ Kocaarslan, "Comparative performance analysis of Artificial Bee Colony algorithm in automatic generation control for interconnected reheat thermal power system," *Int. J. Electr. Power Energy Syst.*, vol. 42, no.1, pp. 167–178, 2012. [\[CrossRef\]](#)



Gauri Sahoo was born in Rourkela, India, in 1981. She received the B.E. degree in Electrical Engineering from the Berhampur University, Odisha, India, in 2004, and the Master's degrees in Electrical Engineering from VSSUT, Burla, Odisha, India in 2009. She is currently working toward the Ph.D. degree at the Department of Electrical and Electronics Engineering, VSSUT, Burla, Odisha, India. Her research interests include Power Electronics, Electrical power system control using artificial intelligence techniques. She is a Life Member of the Indian Society for Technical Education (ISTE).



Rabindra Kumar Sahu received the Ph.D. degree from the Indian Institute of Technology Madras, Chennai, India. He is currently working as Professor in the Department of EEE, Veer Surendrai Sai University of Technology (VSSUT), Burla, Sambalpur, Odisha, India. His research interests include application of soft computing techniques to power system engineering, Flexible AC Transmission Systems (FACTS). Dr. Sahu is life member of ISTE and Fellow of Institution of Engineers (India).



Pratap Chandra Pradhan received the Ph.D. degree from Sambalpur University, Burla, Odisha, India, in 2018, M.E. degree in Power System Engineering from Veermata Jijabai Technological Institute (VJTI), University of Mumbai, India, in 2003. He is currently working as Associate Professor in the Electrical Engineering Department, DRIEMS(Autonomous), Cuttack, Odisha, India. His research interests include the area of Automatic Generation Control, Optimization techniques, Power quality improvements, Distributed generation and development of renewable energy. He is a Fellow of Institution of Engineers (India), Life member of Indian Society for Technical Education (India).



Sidhartha Panda received Ph.D. degree from Indian Institute of Technology (IIT), Roorkee, India, M.E. degree from Veer Surendrai Sai University of Technology (VSSUT). Presently, he is working as a Professor in the Department of Electrical Engineering, Veer Surendrai Sai University of Technology (VSSUT), Burla, Sambalpur, Odisha, India. His areas of research include Flexible AC Transmission Systems (FACTS), Power System Stability, Soft computing, Model Order Reduction, Distributed Generation and Wind Energy. Dr. Panda is a Fellow of Institution of Engineers (India).

## APPENDIX

### Normalized Specification of AC Microgrid

PV:  $K_{PV}=1, T_{PV}=1.8$ ; WTG:  $K_{WTG}=1, T_{WTG}=1$ ; UC:  $K_{UC}=-0.7, T_{UC}=0.9$ ; EV:  $K_{EV}=1, T_{EV}=1$ ; FC:  $K_{FC}=0.01, T_{FC}=4$ ; AE:  $K_{AE}=0.002, T_{AE}=0.5$